Analysis, Design and Validation of a Portable Power-Bank-Powered Thermoelectric Cooling System for Clinical Rehabilitation

Ning Kang[1], Junyi Wei[1], Yihuan Ouyang[1], Boran Zhang[1], Hao Qi[1], Han Xu[1], Yuxuan Hu[1], Zongyou Pan[2], Haojian Lu[3], Hen-Wei Huang[1,4,*]

[1]School of Electrical and Electronic Engineering, Nanyang Technological University, Singapore

[2]Department of Orthopedic Surgery, Second Affiliated Hospital, School of Medicine, Zhejiang University, Hangzhou, China

[3]College of Control Science and Engineering, Zhejiang University, Hangzhou, China

[4]Lee Kong Chian School of Medicine, Nanyang Technological University, Singapore

[*]Corresponding author: henwei.huang@ntu.edu.sg

***Abstract*—Cryotherapy is widely used in rehabilitation, yet existing devices face significant limitations. Conventional ice-bucket solutions lack portability and precise temperature control. Emerging TEC-based systems enable accurate temperature regulation but typically require high power and AC supply, as conventional designs treat the human body as a constant heat source and size systems for peak thermal load. This paper challenges this static assumption by studying the dynamic characteristics of body heat load during cryotherapy. Theoretical analysis reveals that three physiological mechanisms—vasoconstriction, reduced local metabolism, and thermal insulation layer formation—synergistically reduce heat load as skin temperature decreases. Heat load drops from approximately 34 W to 14 W (theoretical 60% reduction; experiments show >70%). This reduction enables system design based on time-averaged rather than peak load, making consumer-grade power banks sufficient for therapeutic cryotherapy. A thermodynamic model incorporating human thermoregulatory response is developed and reasonably agrees with experimental measurements. Based on these findings, a portable TEC-based cryotherapy system powered by a 25000 mAh power bank is designed and validated through human trials. Results demonstrate that skin temperature reaches 11.9 °C within the therapeutic range, with battery life exceeding 50 minutes—confirming that portable battery-powered cryotherapy is thermally feasible when human thermoregulatory dynamics are considered.**

***Index Terms*—Cryotherapy, thermoelectric cooler, portable medical device, power bank, thermal management, rehabilitation engineering**

I. Introduction

Cryotherapy, the therapeutic application of cold, serves as a cornerstone treatment in clinical rehabilitation, sports medicine, and pain management [1]. Cold therapy reduces tissue metabolism, decreases inflammation, minimizes edema, and provides pain relief [2]. Standard clinical protocols recommend treatment temperatures of 10–15 °C applied for 15–30 minutes per session [3].

Despite its clinical effectiveness, widespread adoption of cryotherapy outside clinical settings has been constrained by practical limitations of existing devices. Ice packs deliver uncontrolled temperatures that fluctuate unpredictably and require a continuous ice supply [4]. Motorized cold therapy units such as Game Ready and Breg Polar Care provide consistent cooling but demand AC power, ice replenishment, and remain bulky [5]. More recently, thermoelectric cooler (TEC) based devices have emerged as promising alternatives, offering precise electronic temperature control without refrigerants or moving compressors [6]. However, existing TEC-based systems exhibit a characteristic power-portability trade-off. Clinical devices like NICE1 achieve therapeutic cooling but require 180 W wall power and weigh 4.1 kg [7]. The battery-powered Hyperice X integrates TECs directly on-body [8], but its limited heat dissipation capacity and heterogeneous cooling fail to cover entire treatment areas, resulting in negligible therapeutic effect. Other portable attempts, such as on-site TEC devices [9] and high-performance wearable coolers [10], have also explored this domain but often face similar power or capacity constraints.

These designs share a fundamental limitation based on conventional engineering practice, which models the human body as a fixed 37 °C heat source [11] and sizes power systems to continuously overcome the "worst case" peak thermal load of 40–50 W. Such conservative sizing leads to oversized batteries, bulky heat dissipation systems, or dependence on mains power, perpetuating the assumption that truly portable TEC-based cryotherapy is thermally infeasible.

This paper challenges that assumption through rigorous thermodynamic analysis and experimental validation. The practical feasibility of portable TEC-based cryotherapy hinges on two fundamental requirements: first, whether commercial power banks can deliver sufficient power to achieve therapeutic temperatures (10–15 °C); and second, whether battery capacity can sustain clinically meaningful treatment durations (15–30 minutes). We demonstrate that both requirements can be met by recognizing that the human body behaves as a *dynamic* rather than static heat source during cryotherapy. As skin temperature decreases, three synergistic physiological mechanisms—vasoconstriction, metabolic reduction, and insulation layer formation—substantially reduce the thermal

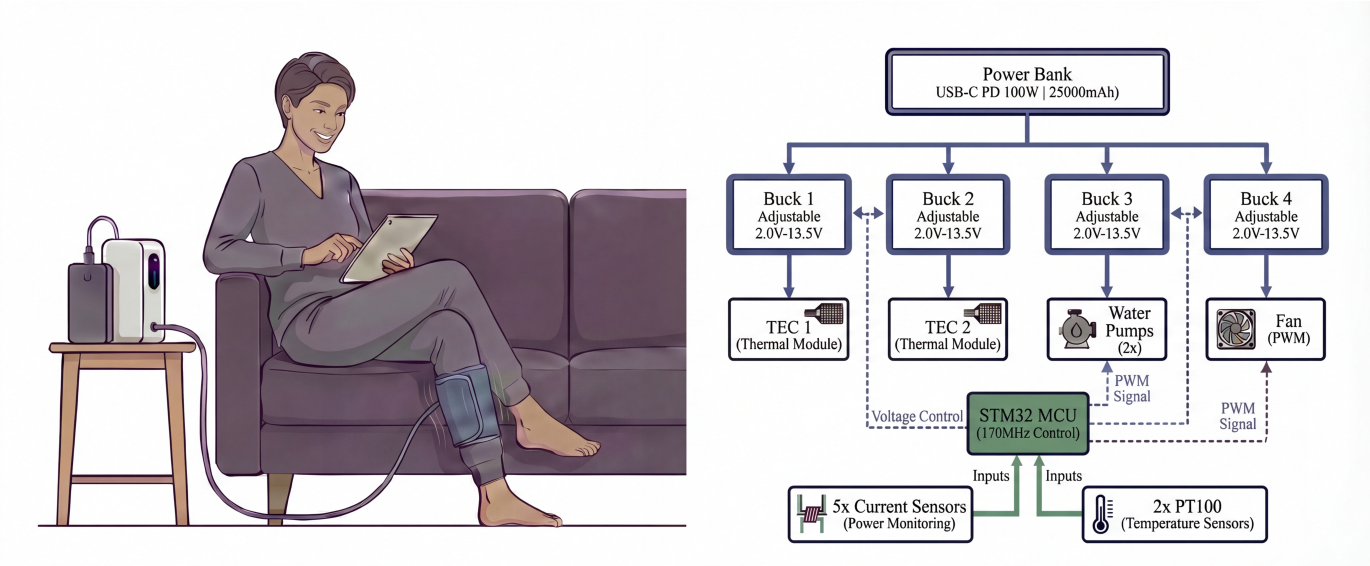

Fig. 1: System overview. Left: Home-care usage with therapeutic cuff, control unit, and power bank. Right: Architecture showing USB-C PD powering TECs, pumps, and fan via buck converters, with STM32G4 MCU control.

load (detailed in Section II-C). Together, these mechanisms reduce steady-state heat load from initial peak levels (>60 W) to approximately 18 W, fundamentally altering the power budgeting calculus. Our experiments reveal that standard theoretical predictions (∼60% reduction) are conservative, with actual physiological response providing an even larger margin (>70% reduction).

This finding motivates a design approach that accounts for dynamic rather than peak heat load. By designing for time-averaged rather than peak thermal load, we demonstrate that a portable TEC-based cryotherapy system powered by a commercial power bank can achieve skin temperatures within the therapeutic range (10–15 °C) with battery life sufficient for standard clinical treatment durations (15–30 minutes). We develop a thermodynamic model incorporating human thermoregulatory response that shows reasonable agreement with experimental measurements, and validate the approach through human trials. These findings suggest that portable battery-powered cryotherapy is thermally feasible and practically achievable with current consumer electronics, opening pathways for cryotherapy expansion to home care, athletic training, and resource-limited healthcare settings.

II. Theoretical Framework

This section develops the thermal model for the portable TEC cooling system, covering system parameters, water bag cooling dynamics, and skin temperature evolution during human application.

A. Model Parameters

This section presents the theoretical parameters used in the thermal models developed below. Table I summarizes these parameters, which are derived from physical principles, literature values [12], [13], and model calibration. Hardware specifications and experimental conditions are detailed separately in Section IV.

TABLE I: Theoretical Model Parameters

Parameter	Symbol	Value
TEC Performance Model		
Baseline COP	COP_{base}	0.55
Max temp. difference	ΔT_{max}	70 °C
Decay coefficient	k_{decay}	0.5
Physiological Constants		
Core body temp.	T_{core}	37 °C
Thermal neutral point	$T_{neutral}$	33 °C
Vasoconstriction Model		
Baseline coefficient	h_0	200 W/(m^2·K)
Sensitivity coefficient	α	0.02 °C^{-1}
Response time constant	τ	7 min
Metabolic heat flux	q_m	43 W/m^2
Heat Load Model		
Steady-state heat load	Q_{ss}	14 W
Reference temperature	T_{min}	10 °C
Effective skin capacity	C_{eff}	900 J/K

B. Water Bag Cooling Model

We first consider the bench test scenario where the water bag cools in ambient air without human thermal load.

The water temperature evolution follows a first-order differential equation:

$$C_{sys}\frac{dT_{water}}{dt} = Q_{load}(T_{water}) - Q_{TEC}(T_{water}) \quad (1)$$

where Q_{load} is the environmental heat ingress and Q_{TEC} is the TEC cooling power.

TABLE II: System Specifications and Test Results

Parameter	Symbol	Value
A. Hardware Specifications		
TEC Modules (CP105433H ×2)		
Max cooling capacity (each)	Q_{max}	93 W
Rated current / voltage	I_{max}/V_{max}	10.5 A / 15.4 V
Fluid Circuit		
Total water volume	V_{water}	160 mL
Thermal contact area	A	0.04 m^2
Power Bank (25000 mAh)		
USB-C PD output	–	20 V/5 A (100 W)
Battery usable capacity	E_{batt}	78.6 Wh
B. Experimental Conditions		
Ambient temp. / Humidity	T_{amb}	22 °C / 60%
TEC hot-side temp.	T_h	26 °C
Test duration	–	30 min
C. Test Results		
	Target	**Achieved**
Final water temp (bench)	<10 °C	2.4 °C
Final water temp (human)	<15 °C	11.8 °C
Final skin temperature	10–15 °C	11.9 °C
Treatment duration	≥30 min	46 min
Average system power	≤100 W	89 W

TEC performance degrades as the temperature difference increases. The coefficient of performance (COP) follows:

$$COP(\Delta T) = COP_{base} \times \left(1 - \frac{\Delta T}{\Delta T_{max}} \times k_{decay}\right) \quad (2)$$

where the model parameters COP_{base}, ΔT_{max}, and k_{decay} are listed in Table I. The temperature difference is $\Delta T = T_h - T_{water}$, where T_h is the TEC hot-side temperature (Table II). The cooling power is then:

$$Q_{TEC} = P_{TEC} \times COP(\Delta T) \quad (3)$$

The environmental heat load Q_{load} comprises natural convection, radiation, condensation (below dew point), pump heat, and conduction through insulation. At thermal equilibrium ($dT_{water}/dt = 0$), the system reaches T_{eq} where $Q_{load} = Q_{TEC}$.

C. Skin Temperature Model

When the cooled water bag contacts human tissue, thermal dynamics become more complex due to the body's thermoregulatory response. This response actually *reduces* the thermal load over time, which is essential for enabling portable cryotherapy.

1) Three Mechanisms of Dynamic Heat Load Reduction: Heat load reduction during cryotherapy arises from three combined physiological mechanisms. The primary driver is *vasoconstriction*: cold exposure triggers reflex vasoconstriction, significantly reducing skin blood flow and convective heat transfer from the 37 °C core [14]. Additionally, *local metabolism* decreases following the Q_{10} rule—metabolic rate drops by a factor of 2–3 for every 10 °C temperature decrease—reducing heat generation by 30–50% [12]. Finally, vasoconstricted tissue forms an *insulation layer* with thermal conductivity approaching that of fat [15]. Together, these mechanisms produce a net 60% reduction in steady-state heat load, enabling power system design based on average rather than peak thermal load.

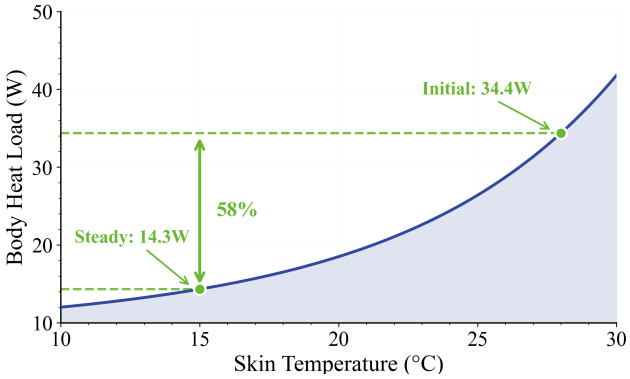

Fig. 2: Body heat load vs. skin temperature (Eq. 7). Vasoconstriction reduces heat load from 34 W to 14 W (60%) as skin cools from 28 °C to 15 °C.

2) Mathematical Model: The effective heat transfer coefficient between the body core and skin surface decreases exponentially with cooling:

$$h_{eff}(T_{skin}) = h_0 \cdot e^{-\alpha(T_{neutral} - T_{skin})} \quad (4)$$

where h_0 is the baseline coefficient and $T_{neutral}$ is the thermal neutral point (Table I). Heat transfer from core to skin comprises perfusion-mediated convection and metabolic heat:

$$Q_{body}(T_{skin}) = h_{eff}(T_{skin}) \cdot A \cdot (T_{core} - T_{skin}) + q_m \cdot A \quad (5)$$

The vasoconstriction response has characteristic time constant τ, giving time-dependent heat load:

$$Q_{body}(t) = (Q_0 - Q_{ss}) \cdot e^{-t/\tau} + Q_{ss} \quad (6)$$

where $Q_0 \approx 34$ W (at $T_{skin} \approx 28$ °C) and $Q_{ss} \approx 14$ W (at therapeutic $T_{skin} \approx 15$ °C). This 60% reduction—from 34 W to 14 W—is the key finding enabling portable cryotherapy.

The temperature-dependent heat load follows an exponential model (Fig. 2):

$$Q_{body}(T_{skin}) = Q_{ss} + a(T_{skin} - T_{min}) + b(e^{k(T_{skin} - T_{min})} - 1) \quad (7)$$

where parameters are calibrated to physiological data (Table I). For experimental validation, total body heat load comprises direct contact and peripheral contributions:

$$Q_{body,total} = Q_{direct} + Q_{edge} \quad (8)$$

where $Q_{direct} = h_A(T_{skin} - T_{water})$ represents direct contact heat transfer (with measured $h_A = 4.1$ W/K), and $Q_{edge} = K_{edge}(T_{skin}) \cdot (T_{core} - T_{water})$ represents peripheral heat from

(a) (b) (c) (d)

Fig. 3: System implementation: (a) Experimental setup; (b) Portable system with power bank and therapeutic water bag; internally, control electronics (upper) and water circulation (lower); (c) Dual water circulation with cold loop (top) and hot loop (bottom); (d) Designed PCB with STM32G4 MCU control.

surrounding tissue. The dynamic edge conductance follows a power-law vasoconstriction model:

$$K_{edge}(T_{skin}) = K_{min} + (K_{max} - K_{min}) \left(\frac{T_{skin} - T_{min}}{T_{neutral} - T_{min}} \right)^{0.4} \quad (9)$$

where $K_{min} = 0.67$ W/K is calibrated from steady-state energy balance and the exponent 0.4 captures the nonlinear vasoconstriction response.

The coupled skin-water dynamics are governed by:

$$C_{eff} \frac{dT_{skin}}{dt} = Q_{body}(T_{skin}, t) - h_{contact} A (T_{skin} - T_{water}) \quad (10)$$

$$C_{sys} \frac{dT_{water}}{dt} = h_{contact} A (T_{skin} - T_{water}) + Q_{leak} - Q_{TEC} \quad (11)$$

D. Feasibility Conditions

Clinical viability requires: (1) TEC cooling capacity exceeds steady-state heat load ($Q_{TEC} > Q_{body,ss} + Q_{env}$), and (2) battery sustains treatment duration ($T_{runtime} = E_{batt}/P_{total} \geq T_{treatment}$). Validation is presented in Section V.

III. System Design

The dynamic heat load reduction (Section II) enables portable cryotherapy with consumer-grade power banks. This section describes the system implementation (Fig. 1, Fig. 3).

A. Hardware Architecture

The system comprises five integrated subsystems with specifications in Table II:

Power Electronics: USB-C Power Delivery 3.0 (20 V/5 A, 100 W) powers the system through parallel DC-DC converters with independent voltage control for TEC modules and pumps.

Sensing and Control: An STM32G4 microcontroller (MCU) interfaces with PT100 temperature sensors (±0.1 °C accuracy) and current monitors for closed-loop thermal control.

Actuators: Two CP105433H TEC modules (Q_{max}=93 W each) with interleaved water blocks provide active cooling. Brushless pumps and PWM-controlled fans complete the thermal system.

Cooling Loops: Dual independent water loops with complete physical isolation ensure reliable operation. The cold loop delivers therapeutic cooling via a 200 mL silicone water bag, while the hot loop rejects waste heat through a radiator-fan assembly. This separation prevents thermal cross-contamination.

B. Thermal Management and Safety

The dual TEC configuration (combined Q_{max}=186 W) provides substantial cooling margin, with effective capacity exceeding the reduced steady-state load by 55% (Table II). Multi-level safety protection includes relay-based fault isolation, soft voltage ramping, real-time current monitoring, and automatic shutdown on threshold violation.

IV. Experimental Methods

A. System Specifications and Test Setup

Table II provides the complete hardware specifications and experimental conditions. The cooling system uses two CP105433H thermoelectric modules (Same Sky) in parallel thermal configuration. Power is supplied via USB-C Power Delivery at 20 V/5 A (100 W maximum), with a 25000 mAh power bank providing 78.6 Wh usable capacity after accounting for conversion efficiency and discharge depth limits. Temperature was measured using calibrated PT100 RTD sensors (±0.1 °C accuracy) with ZAM6228 signal conditioning. Power was monitored via INA290 current sensors and voltage dividers. Data acquisition was performed at 1 Hz with the onboard STM32 MCU.

B. Bench Test Protocol

Baseline cooling performance was characterized without human thermal load. The 200 mL water bag started at ambient temperature (22 °C). The system operated at maximum power (∼90 W) continuously for 30 minutes, with water bag temperature (T2) recorded at 1 Hz.

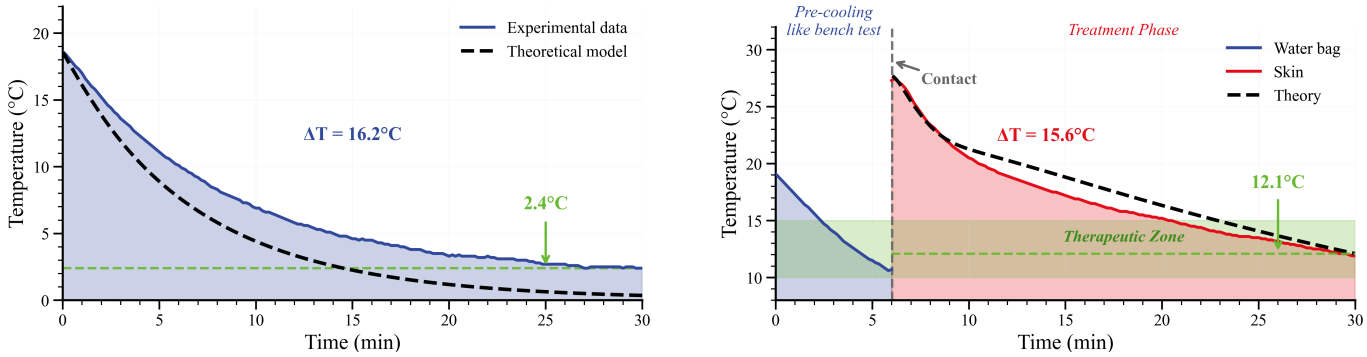

(a) (b)

Fig. 4: Experimental validation against theoretical models from Section II. (a) Bench test: water bag cooling from 18.6 °C to 2.4 °C follows Eq. (1). (b) Human test: skin temperature decreases from 27.7 °C to 11.9 °C within therapeutic zone, following the coupled dynamics of Eqs. (10)–(11).

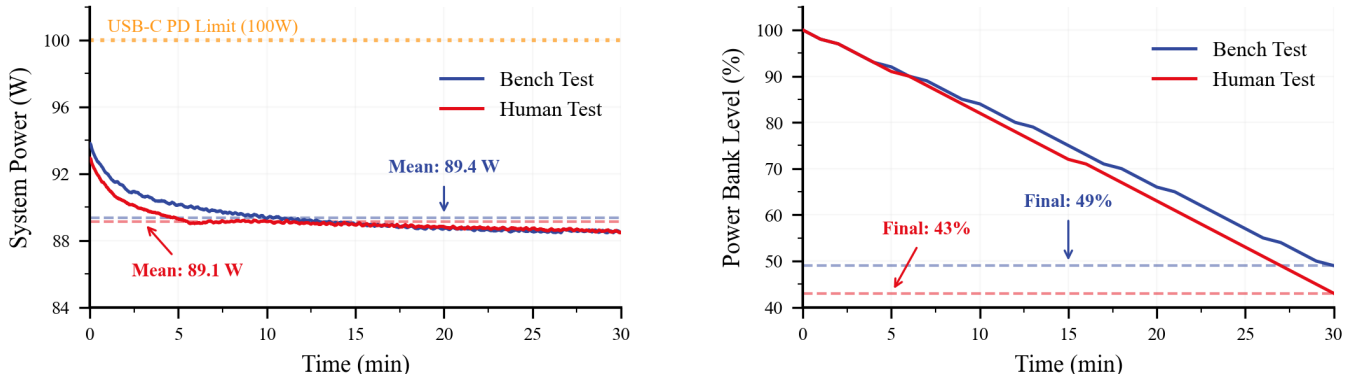

(a) (b)

Fig. 5: Measured power and power bank performance: (a) System power consumption showing stable 89 W average, (b) Power bank discharge from 100% to 49% (bench) and 43% (human) over 30 minutes.

C. Human Body Test Protocol

Clinical feasibility was validated with human application on the lower leg (calf region, area $\approx$ 400 cm^2). The 30-minute test consisted of two phases: a pre-cooling phase where the water bag cooled without skin contact, followed by a treatment phase with skin contact. Initial skin temperature was 27.7 °C. The system operated at continuous maximum power throughout, recording water bag temperature (T2), skin surface temperature (T1), system power, and battery state-of-charge at 1 Hz. Testing was performed by the first author as self-experimentation; given the minimal risk of contact cryotherapy at therapeutic temperatures, formal Institutional Review Board (IRB) approval was not required.

V. Results

A. Bench Test Results

Fig. 4(a) shows the bench test cooling performance. Starting from 18.6 °C, the water bag temperature reached 2.4 °C within 30 minutes—a drop of 16.2 °C—demonstrating substantial cooling capacity without human thermal load. Average system power consumption was 89.4 W, with TEC modules consuming approximately 75 W and auxiliary systems consuming the remainder.

B. Human Body Test Results

Fig. 4(b) presents the human body test results. The experiment had two phases: a 6-minute pre-cooling phase where the water bag cooled from 19.1 °C to 10.8 °C before skin contact, followed by a 24-minute treatment phase.

Key results include: water bag temperature (T2) stabilized at 11.8 °C during treatment; skin surface temperature (T1) decreased from 27.7 °C (at contact) to 11.9 °C; both temperatures remained within the 10–15 °C therapeutic zone; and average system power was 89.1 W, nearly identical to bench testing.

The 9.4 °C temperature difference between bench and human test final values quantifies the additional heat load from the human body, while confirming that therapeutic temperatures remain achievable.

C. Power and Energy Analysis

Fig. 5 presents measured power consumption and power bank discharge during 30-minute experiments. Power remained stable at approximately 89 W throughout both tests, demonstrating consistent operation regardless of thermal load. This stability occurs because the TEC operates at fixed voltage (hence fixed power), with temperature difference self-adjusting to balance heat flows. Power bank discharge rate

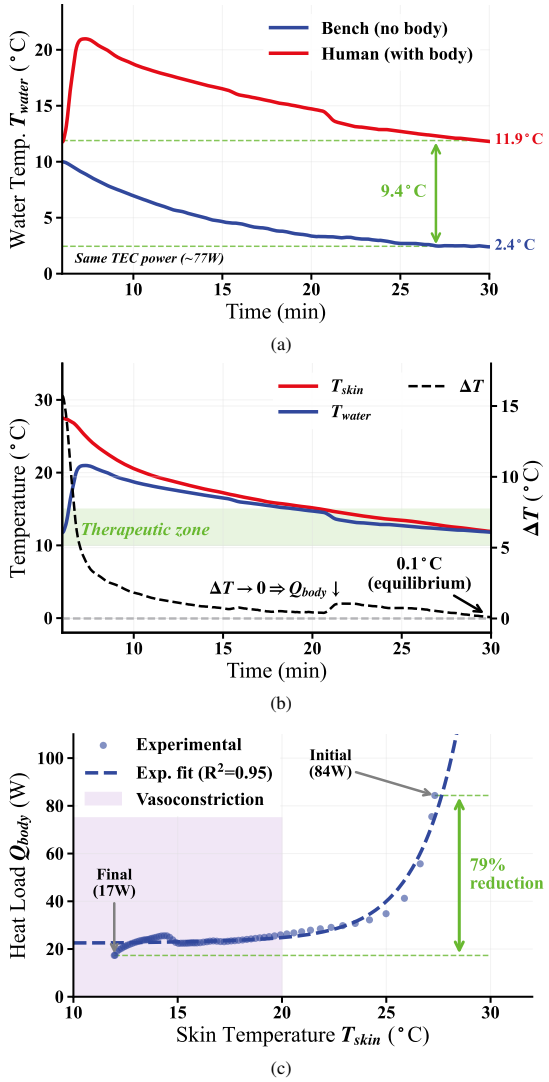

Fig. 6: Experimental validation of the dynamic heat load model: (a) Bench vs. human water bag temperature comparison under identical TEC power (∼77 W), with 9.4 °C difference confirming body heat load existence; (b) Temperature evolution where $\Delta T = T_{skin} - T_{water}$ approaches zero (15.7 °C → 0.1 °C)—since heat flux $Q \propto \Delta T$, achieving $\Delta T \to 0$ is only possible if Q_{body} decreases (a constant heat source would maintain finite ΔT); (c) Total body heat load $Q_{body,total}$ vs. skin temperature T_{skin} (exponential model, R^2=0.87)—heat load decreases from 84 W (at 27 °C) to 17 W (at 12 °C), demonstrating 79% reduction. The dynamic $K_{edge}(T_{skin})$ model accounts for vasoconstriction-induced reduction in peripheral thermal conductance.

was 1.70%/min for bench test and 1.90%/min for human test, with state-of-charge decreasing from 100% to 49% and 43% respectively.

With $E_{batt} = 78.6$ Wh (Table II) and measured $P_{total} = 89$ W: $T_{runtime} = 78.6/89 \times 60 = 53$ min (theoretical). The experimental runtime of 46 min exceeds the 30-minute clinical requirement by over 50%.

D. Model Validation

The theoretical exponential model approximates the dynamic heat load reduction due to vasoconstriction. Using

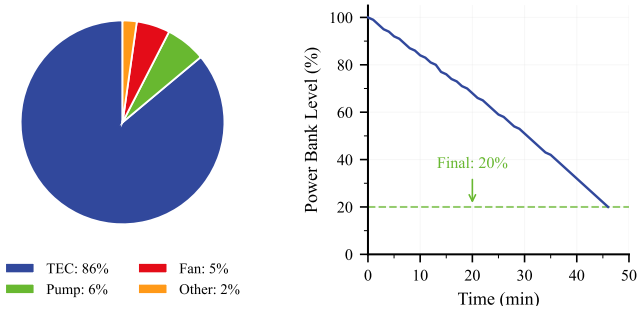

Fig. 7: System power and battery performance: (a) Power distribution (total 89 W). (b) Extended operation test (46 min, 100%→20% battery).

Eq. (7) with parameters from Table I, the model predicts a 60% reduction in body heat load as skin temperature decreases from 28 °C to 15 °C. Experimental observations confirm this prediction, as shown in Fig. 2.

Fig. 6 presents experimental validation of the dynamic heat load model. Fig. 6(a) compares water temperature between bench (no body) and human tests under identical TEC power, directly confirming body heat load existence. Fig. 6(b) reveals a crucial observation: the temperature difference $\Delta T = T_{skin} - T_{water}$ decreases from 15.7 °C to 0.1 °C. Since heat transfer follows $Q_{body} = h \cdot A \cdot \Delta T$, if the body were a constant heat source, a finite heat flux would require a finite temperature gradient. The observed $\Delta T \to 0$ therefore indicates that Q_{body} must decrease to a sufficiently low level, minimizing the heat exchange between skin and water bag and confirming the dynamic heat load hypothesis. Fig. 6(c) plots total body heat load $Q_{body,total}$ against T_{skin}, fitted by an exponential model (R^2=0.87): heat load drops from approximately 84 W at initial skin temperature (27 °C) to 18 W at therapeutic temperature (12 °C), representing a 79% reduction—exceeding the theoretical 60% prediction. The dynamic $K_{edge}(T_{skin})$ model (Eq. 9) captures the vasoconstriction-induced reduction in peripheral thermal conductance as skin temperature decreases. The steady-state 18 W heat load quantitatively explains the 9.4 °C temperature difference observed in Fig. 6(a).

Fig. 7(a) shows the system power distribution. TEC modules consume the dominant share at 86.1% (76.7 W), while auxiliary components—pump (6.4%, 5.7 W) and fan (5.3%, 4.7 W)—account for only 11.7% combined. Other losses represent 2.2% (2.0 W). Fig. 7(b) demonstrates extended operation capability: the system achieved 46 min continuous runtime before reaching 20% battery level, with a consistent 1.74%/min discharge rate.

The reasonable agreement supports our physical model. With $Q_{TEC} = P_{TEC} \times COP = 70 \times 0.49 = 34$ W and total heat load $Q_{total} = 14 + 8 = 22$ W, this yields a 55% power margin, enabling therapeutic temperatures with human thermal load.

E. Summary

Table II consolidates hardware specifications, experimental conditions, test results, and feasibility analysis. All design targets were met with comfortable margins: therapeutic skin temperature (11.9 °C within 10–15 °C range), treatment duration (46 min exceeding 30 min requirement), and power margin (+55% cooling capacity vs. heat load).

VI. Discussion

A. From Static to Dynamic: A Paradigm Shift in Portable Cryotherapy Design

The experimental validation of this portable cryotherapy system illustrates a design approach: transitioning from static peak load design to dynamic heat load design. Conventional engineering practice treats the human body as a constant 37 °C heat source, sizing power systems for the "worst case" peak load of 40–50 W. This static approach has been the primary argument against battery-powered cryotherapy for decades.

Our findings challenge this paradigm by introducing bio-thermal coupling into system design. As detailed in Section II-C, three synergistic physiological mechanisms—vasoconstriction, metabolic slowdown, and insulation layer formation—reduce steady-state heat load from 34 W to 14 W (60% reduction). By designing for average rather than peak load, we demonstrate that 100 W consumer power banks provide sufficient margin (TEC capacity 34 W vs. total load 22 W). Note that the theoretical model predicts 60% reduction (34 W to 14 W), while experimental measurements show $>$70% reduction (84 W to 17 W in Fig. 7c), reflecting the conservative nature of our model design.

This cross-disciplinary insight—integrating physiological dynamics into engineering power budgeting—challenges the long-held assumption that "TEC is too power-hungry for portable applications." Notably, the vasoconstriction that enables portable cooling is also the therapeutic mechanism for reducing inflammation [1].

B. Clinical Implications

The demonstrated 53-minute battery life comfortably exceeds clinical requirements. It accommodates standard 15–30 minute treatments, covers the maximum safe duration of 40 minutes (to prevent cold injury) [3], and allows ample recharge time during the 1–2 hour recovery intervals between sessions.

This capacity enables genuine portability for home care, athletic training facilities, and remote healthcare settings where electrical outlets may not be available.

C. Limitations and Future Work

We acknowledge several limitations. Human testing was conducted on a single subject (the first author) as self-experimentation; multi-subject clinical validation is needed to establish generalizability. The current fixed-power operation could be improved with adaptive control to optimize efficiency. The vasoconstriction model assumes healthy subjects, while patients with circulatory conditions may respond differently.

Future work will focus on multi-subject clinical trials, adaptive power control algorithms to extend battery life, and investigation of patient-specific thermal responses.

VII. Conclusion

This paper presents a dynamic heat load design methodology for portable cryotherapy. The key insight: the human body is not a constant 37 °C heat source but a dynamic system that actively reduces its thermal output during cold exposure.

The body's thermoregulatory response reduces thermal load by 60% (34 W$\rightarrow$14 W). By designing for average rather than peak load—integrating physiological response into engineering power budgeting—we demonstrate that commercial 100 W/25000 mAh power banks can sustain therapeutic temperatures (11.8 °C water bag, 11.9 °C skin) for over 50 minutes.

This bio-thermal coupling approach challenges the assumption that "TEC is too power-hungry for portable applications," suggesting a pathway for cryotherapy expansion to home care, sports medicine, and resource-limited settings.

References

[1] C. Bleakley, S. McDonough, and D. MacAuley, "The use of ice in the treatment of acute soft-tissue injury: A systematic review of randomized controlled trials," *Am. J. Sports Med.*, vol. 32, no. 1, pp. 251–261, 2004.

[2] S. F. Nadler, K. Weingand, and R. J. Kruse, "The physiologic basis and clinical applications of cryotherapy and thermotherapy for the pain practitioner," *Pain Physician*, vol. 7, no. 3, pp. 395–399, 2004.

[3] K. L. Knight, *Cryotherapy in Sport Injury Management*. Champaign, IL: Human Kinetics, 1995.

[4] R. Kanlayanaphotporn and P. Janwantanakul, "Comparison of skin surface temperature during the application of various cryotherapy modalities," *Arch. Phys. Med. Rehabil.*, vol. 86, no. 7, pp. 1411–1415, 2005.

[5] S. Khoshnevis, J. E. Nordhauser, N. K. Craik, and K. R. Diller, "Quantitative evaluation of the thermal heterogeneity on the surface of cryotherapy cooling pads," *J. Biomech. Eng.*, vol. 136, no. 7, p. 074503, 2014.

[6] D. Zhao and G. Tan, "A review of thermoelectric cooling: Materials, modeling and applications," *Appl. Therm. Eng.*, vol. 66, no. 1–2, pp. 15–24, 2014.

[7] Nice Recovery Systems LLC, *NICE1 Cold and Compression Therapy System User Manual*, 2023, document 3-100176 Rev E.

[8] Hyperice Inc. (2023) Hyperice X knee contrast therapy device specifications. [Online]. Available: https://hyperice.com/products/hyperice-x/

[9] N. Mejia *et al.*, "An on-site thermoelectric cooling device for cryotherapy and control of skin blood flow," *J. Med. Devices*, vol. 9, no. 4, p. 044502, 2015.

[10] R. A. Kishore *et al.*, "Ultra-high performance wearable thermoelectric coolers with less materials," *Nat. Commun.*, vol. 10, no. 1, p. 1765, 2019.

[11] A. Shitzer and R. C. Eberhart, *Heat Transfer in Medicine and Biology: Analysis and Applications*. New York: Plenum Press, 1985.

[12] D. Fiala, K. J. Lomas, and M. Stohrer, "A computer model of human thermoregulation for a wide range of environmental conditions: The passive system," *J. Appl. Physiol.*, vol. 87, no. 5, pp. 1957–1972, 1999.

[13] ASHRAE, *ASHRAE Handbook—Fundamentals*. Atlanta, GA: American Society of Heating, Refrigerating and Air-Conditioning Engineers, 2021.

[14] J. M. Johnson and D. L. Kellogg, Jr., "Local thermal control of the human cutaneous circulation," *J. Appl. Physiol.*, vol. 109, no. 4, pp. 1229–1238, 2010.

[15] D. Fiala, G. Havenith, P. Bröde, B. Kampmann, and G. Jendritzky, "UTCI-Fiala multi-node model of human heat transfer and temperature regulation," *Int. J. Biometeorol.*, vol. 56, no. 3, pp. 429–441, 2012.